Multiple inhibitory ligands induce impaired T-cell immunologic synapse function in chronic lymphocytic leukemia that can be blocked with lenalidomide: establishing a reversible immune evasion mechanism in human cancer

Alan G. Ramsay,[1] Andrew J. Clear,[1] Rewas Fatah,[1] and John G. Gribben[1]

[1]Centre for Haemato-Oncology, Barts Cancer Institute, Queen Mary University of London, London, United Kingdom

Cancer immune evasion is an emerging hallmark of disease progression. We have demonstrated previously that impaired actin polymerization at the T-cell immunologic synapse is a global immune dysfunction in chronic lymphocytic leukemia (CLL). Direct contact with tumor cells induces defective actin polarization at the synapse in previously healthy T cells, but the molecules mediating this dysfunction were not known. In the present study, we show via functional screening assays that CD200, CD270, CD274, and CD276 are coopted by CLL cells to induce impaired actin synapse formation in both allogeneic and autologous T cells. We also show that inhibitory ligand–induced impairment of T-cell actin dynamics is a common immunosuppressive strategy used by both hematologic (including lymphoma) and solid carcinoma cells. This immunosuppressive signaling targets T-cell Rho-GTPase activation. Of clinical relevance, the immunomodulatory drug lenalidomide prevented the induction of these defects by down-regulating tumor cell–inhibitory molecule expression. These results using human CLL as a model cancer establish a novel evasion mechanism whereby malignant cells exploit multiple inhibitory ligand signaling to down-regulate small GTPases and lytic synapse function in global T-cell populations. These findings should contribute to the design of immunotherapeutic strategies to reverse T-cell tolerance in cancer. (*Blood*. 2012;120(7):1412-1421)

Introduction

Targeted immunotherapy has the potential to affect cancer treatment and target drug-resistant tumor subclones.[1] Chronic lymphocytic leukemia (CLL) is a good model with which to test novel immunotherapeutic approaches[2] and to examine tumor cell interactions with immune cells.[3] The intrinsic nature of CLL and other leukemias means that circulating T cells and tumor cells are in regular contact interactions. Our previous gene-expression profiling studies in peripheral blood $CD4^+$ and $CD8^+$ T-cell populations from CLL patients revealed profound dysregulation in multiple gene pathways, including the actin cytoskeleton.[4] Functional T-cell immunologic synapses control assembly of signaling complexes between the Ag-ligated TCR and the cytoskeletal signaling layer, and is dependent on polymerized filamentous actin (F-actin).[5] T cells isolated from CLL patients have defective F-actin polymerization and immune synapse formation at the contact site with APCs, steps required for activation and CTL effector function.[6,7] Direct contact with CLL tumor cells induces these molecular and functional defects in previously healthy T cells in vitro and in vivo.[4,6,8] This tumor-immunosuppressive mechanism likely contributes to disease progression and blocks the effectiveness of current immunotherapy approaches. Therefore, it is essential to elucidate the signaling mechanisms mediating T-cell dysfunction in CLL to improve our understanding of how cancer cells evade immune recognition and then use this knowledge to improve immunotherapy strategies.

In the present study, we used human CLL as a model cancer to define a novel cancer immune evasion mechanism whereby tumor cells exploit the normally tightly regulated inhibitory signaling axes of multiple cell-surface–inhibitory molecules to down-regulate Rho-GTPase activation signaling, actin polymerization, and lytic synapse function in global T-cell populations.

Methods

Cell isolation and culture

All primary patient and age-matched healthy donor samples were obtained after written consent in accordance with the Declaration of Helsinki, and were approved by the North London Research Ethics Committee. All CLL patients (n = 68) were previously untreated (median time from diagnosis, 30 months [range 6-96]) at the time that heparinized venous blood samples were obtained for these studies. In vivo lenalidomide-derived samples came from a review board–approved clinical trial examining the efficiency of lenalidomide in previously treated symptomatic CLL patients. We used healthy allogeneic B cells as controls. Peripheral blood and lymph node samples were obtained from untreated follicular lymphoma (FL; n = 6) and transformed diffuse large B-cell lymphoma (transformed DLBCL or t-FL; n = 6) patients undergoing diagnostic biopsies. These nonleukemic phase FL samples had no immunophenotypic evidence of peripheral blood disease involvement. Peripheral blood T cells were isolated from the same patients from whom the lymph node biopsies were available. FL patients were selected to represent the heterogeneity of the disease, including clinical grade (grades 1, 2, and 3A) and stage of disease. Clinical factors were not shown to be associated with extent of B7-related ligand immunosuppressive signaling activity. Patient- and age-matched healthy donor mononuclear cells were separated by

Submitted February 16, 2012; accepted April 23, 2012. Prepublished online as *Blood* First Edition paper, April 30, 2012; DOI 10.1182/blood-2012-02-411678.

The online version of this article contains a data supplement.

The publication costs of this article were defrayed in part by page charge payment. Therefore, and solely to indicate this fact, this article is hereby marked "advertisement" in accordance with 18 USC section 1734.

Ficoll-Hypaque density gradient centrifugation. Healthy donor lymphocytes for the coculture assays were obtained from buffy coats prepared by the National Blood Service, NHS Blood and Transplant (Brentwood, United Kingdom). $CD3^+$ and $CD8^+$ T cells were negatively selected using Miltenyi Biotec magnetic-activated cell sorting (MACS) cell isolation kits. Normal and malignant B cells were positively selected using MACS $CD19^+$ microbeads. An autoMACS Pro separator (Miltenyi Biotec) was used for the gentle cell sorting of viable, functionally active cells. The total number of purified FL or DLBCL cells after isolation and purification ranged between 1×10^8 and 5×10^8 cells depending on the size of lymph node biopsy material available. The purity of isolated lymphocytes was always $> 95\%$ as determined by flow cytometry. Cell numbers and viability were measured using a Vi-CELL XR analyzer (Beckman Coulter). Primary cells were maintained in RPMI 1640 medium containing 10% human serum. MEC1 cells were cultured in IMDM GlutaMAX (Invitrogen); SKOV3 cells in DMEM high-glucose medium; VB6 cells in keratinocyte growth medium[9]; and RPMI8226, U266, DoHH2, and CRL cells in RPMI 1640 medium. All culture media contained 10% (vol/vol) FBS, 100 U/mL of penicillin, and 100 μg/mL of streptomycin and were kept at 37°C with 5% CO_2. The telomerase-immortalized benign human ovarian cell line IOSE was cultured in MCDB105/199 (1:1) medium with 15% FBS/epidermal growth factor (10 ng/mL)/hydrocortisone (0.5 μg/mL)/insulin (5 μg/mL)/bovine pituitary extract (34 μg protein/mL).[10]

Customized siRNA library screen

MEC1 cells were treated with Accell siRNA SMARTpool-targeted reagents (Dharmacon) according to the manufacturer's delivery protocol. Briefly, 1×10^5 MEC1 cells were incubated with siRNA (0.5μM) in 96-well format at 37°C with 5% CO_2 for 72 hours before these cells were pooled (1×10^6) and used in coculture assays with healthy donor T cells (3×10^6). Accell medium alone did not affect the viability of MEC1 cells. Primary CLL cells were nucleofected (Nucleofector Transfection Program V06; Amaxa) with siRNA SMARTpool-targeted reagents (Dharmacon). Efficiency of siRNA uptake, as estimated with green (dye) nontargeting siRNA and fluorescent microscopy, was $> 80\%$ (MEC1 cells) and 40%-60% (CLL cells). The levels of target protein as measured by FACS mean fluorescence intensity (MFI) were reduced by 70%-80% in MEC1 cells and by 50%-60% in CLL cells after siRNA treatment.

Abs and reagents

Dynabeads human T-activator CD3/CD28 and control Dynabeads Pan mouse IgG, DynaMag-2, Pooled AB human serum, penicillin-streptomycin, rhodamine phalloidin, CellTracker Blue CMAC (7-amino-4-chloromethylcoumarin), and Alexa Fluor 488–labeled goat anti–rabbit Ab were all from Life Technologies. Trypsin-EDTA was from PAA. Functional grade CD200 (clone 325531), CD200 receptor (R), and CD54 (clone HA58) neutralizing Abs were obtained from R&D Systems. CD274 (clone MIH1), CD276 (clone MIH35), CD272 (clone MIH26), and CD279 (clone J116) neutralizing Abs were from eBiosciences. CD270 neutralizing Ab (clone 122) was from LifeSpan BioSciences. Anti-granzyme B Ab was from Abcam. Phospho-myosin light-chain Ab was from Cell Signaling Technology.

Flow cytometry

We performed flow cytometry on an LSRFortessa cell analyzer (BD Biosciences) and analyzed data using FlowJo Version 8.8.6 software (TreeStar). We gated live cells by forward and side scatter, DAPI negative staining, and ensured correct compensation and acquisition setup. Cells were resuspended at 1×10^6 in 100 μL of PBS containing 2% human serum. We incubated cells with pretitrated Abs to cell-surface markers at 4°C for 20 minutes. CD200 (clone 325516, PE), CD276 (clone 185504) were from R&D Systems; CD200 receptor (R; clone OX108, PE), CD270 (clone eBioHVEM-122, PE), CD274 (clone MIH1, PE), and CD279 (clone MIH4, PE) were from eBiosciences. CD272 (clone J168-540, PE) and the appropriate isotype controls were from BD Biosciences. The experiment shown in Figure 2B was performed on freshly purified $CD19^+$ (CLL cells compared with age-matched healthy donor B cells) or $CD3^+$ T-cell populations (from autologous CLL patient cells compared with age-matched healthy donors). The experiment shown in Figure 4B was performed by coculturing freshly purified $CD19^+$ cells (CLL cells or age-matched healthy donor B cells) with $CD3^+$ T cells and using CD3 (clone UCHT1, FITC) to analyze the expression of PE-conjugated Abs in gated cell populations at baseline and after 48 hours of incubation with lenalidomide or vehicle control. Results are expressed as the proportion of cells expressing antigens of interest (percent positive staining) or MFI corrected for nonspecific background staining (isotype control-PE).

TMA, IHC, and image analysis

Tumor tissue microarrays (TMAs) from Barts and The London School of Medicine and Dentistry (London), including a reactive lymph node TMA ($n = 30$ patient samples), were used and analyzed by immunohistochemistry (IHC). CLL lymphoid TMAs were constructed from initial diagnostic lymph nodes (71 patient samples).[11] CLL patients were selected as representative of the heterogeneity of the disease, including different Rai stages (I-III) and immunoglobulin variable heavy chain mutation status (mutated and unmutated; data not shown). In a separate TMA, representative extremes of survival were used, including a group of 17 poor-prognosis patients whose median survival was 38 months (with all patients dying of their disease) and a group of 18 patients with a longer median survival of > 10 years.[12] Extremes of survival diagnostic FL TMAs consisted of 34 samples from patients whose survival was less than 5 years and 25 samples from patients whose survival was more than 15 years from diagnosis.[13] Patients who lived less than 5 years from diagnosis (the short-survival group) had a median survival of 2 years and all died as a result of their disease. Patients who lived more than 15 years from diagnosis (the long-survival group) had a median survival of 21 years. We also examined TMAs before and after transformation (35 patients with paired samples).[14] CD200 (Prestige Antibodies; Sigma-Aldrich), CD274 (ab82059, Abcam), CD276 (Prestige Antibodies; Sigma-Aldrich), and CD270 (ab89479; Abcam) staining on $CD20^+$ (Novocastra) tumor B cells (cancer TMAs) or nonmalignant B cells (reactive TMAs) and CD279 (ab52597, NAT; Abcam) and CD272 (ab96560; Abcam) staining on $CD3^+$ T cells (Novocastra) were evaluated for mean intensity expression using automated IHC expression with serial section overlay analysis to identify cell-specific staining (Ariol Automated Image Analysis System; Applied Imaging).

Primary coculture screening assays

To analyze the impact on T cells of hematologic tumor cell direct contact, T cells (5×10^6/mL) and tumor cells (1×10^7/mL; or healthy donor B cells) were cocultured together (1:2 ratio) in full culture medium for 48 hours in a 24-well culture plate. Autologous CLL coculture assays were set up in a 1:10 T-cell to tumor-cell ratio. For functional screening assays, T cells were cocultured with tumor cells (or healthy donor B cells) that had been pretreated with individual or pooled neutralizing (10 μg/mL) Abs for 1 hour and subsequently washed to remove any unbound Ab. All experiments were performed using isotype-matched IgG as controls. After coculture, cells were harvested and T cells isolated by negative selection (using MACS CD20 and CD19 microbeads) for subsequent viability (Vi-CELL XR analyzer $> 90\%$), flow cytometry purity analysis ($> 95\%$), and subsequent functional assays. To analyze the impact on T cells of solid epithelial cancer cell line direct contact, T cells (5×10^6/mL) were cocultured together with a confluent monolayer of cells (1:1 ratio) in full culture medium for 24 hours in a 6-well culture plate. For functional screening assays, adherent cells had been pretreated with individual or pooled neutralizing Abs (10 μg/mL) for 1 hour and subsequently washed to remove any unbound Ab. After coculture, suspension T cells were harvested for subsequent viability analysis ($> 90\%$) and subsequent functional assays.

T-cell to APC-cell conjugation assays

Briefly, healthy or malignant B (CLL) cells (2×10^6) were stained with CellTracker Blue CMAC following the manufacturer's instructions and pulsed with or without 2 μg/mL of a cocktail of staphylococcal superantigens (sAgs; SEA and SEB; Sigma-Aldrich) for 30 minutes at 37°C. B cells were centrifuged at 200*g* for 5 minutes with an equal number of T cells

(purified from primary coculture) and incubated at 37°C for 10 minutes ($CD8^+$ T cells) or 20 minutes ($CD3^+$ T cells). Cells were transferred onto microscope slides (Menzel-Glaser Polysine slides; Thermo Scientific) using a cell concentrator (Cytofuge 2) and fixed for 15 minutes at room temperature with 3% methanol-free formaldehyde (TABB Laboratories) in PBS.

Immunofluorescence labeling and confocal microscopy

Immunofluorescent labeling was done using Cytofuge2 cell concentrator units, which allows meticulous experimental handling. Briefly, cells were permeabilized with 0.3% Triton X-100 (Sigma-Aldrich) in PBS for 5 minutes and treated for 10 minutes with 0.1% BSA in PBS blocking solution. Primary and secondary Abs were applied sequentially for 45 minutes at 4°C in 5% goat serum (Sigma-Aldrich) in PBS blocking solution. F-actin was stained with rhodamine phalloidin following the manufacturer's instructions applied alone or with the secondary Ab. After washing, the cell specimens were sealed with 22- × 32-mm coverslips using fluorescent mounting medium (Dako). The specificity of staining was optimized and controlled using appropriate dilutions of isotype-control primary Abs and subsequent fluorescent secondary Abs. Background staining with control Abs was compared with positively stained cells and was not visible using identical acquisition settings. Medial optical section images were captured with a Zeiss 510 confocal laser-scanning microscope using a 63×/1.40 oil objective and LSM Version 3.2 SP2 imaging software (Zeiss). Detectors were set to detect an optimal signal below saturation limits. Fluorescence was acquired sequentially to prevent passage of fluorescence from other channels (Multi-Track). Image sets to be compared were acquired during the same session using identical acquisition settings.

Quantitative image analysis of F-actin polymerization at T-cell synapses. Blinded confocal images (n = 10 per patient treatment group) were analyzed using AxioVision Version 4.8 image analysis software (Zeiss). T-cell/APC conjugates were identified only when T cells were in direct contact interaction with APCs (blue fluorescent channel). The AxioVision area analysis tool was then used to measure the total area (in square micrometers) of F-actin (red fluorescent channel) accumulation at all T-cell contact sites and synapses with APCs (minimum n = 100 per patient treatment group). These data were then exported into Prism Version 5 software (GraphPad) for statistical analysis and to generate a mean area value per experimental population. Rapid functional screening results and verification of any gain in function using our synapse bioassay was performed using a customized automatic analysis macro with high-throughput screen Cellomics technology (ASSAYbuilder; Zeiss) that measured the area (in square pixels) of F-actin polymerization at each T-cell/APC contact site with batch analysis (data not shown).

CTL cytotoxicity assay

$CD8^+$ CTL cytolytic activities were determined using the CytoTox 96 NonRadioactive Cytotoxicity Assay (Promega). Briefly, after primary coculture, CTLs were incubated with APC target cells (third-party healthy donor B cells or autologous CLL cells pulsed with sAg) at a 30:1 effector-to-target ratio at 37°C for 4 hours. The percent cytotoxicity for each treatment was calculated according to the manufacturer's instructions as follows: (experimental − effector cell spontaneous LDH release − target spontaneous)/(target cell maximum − target cell spontaneous) × 100.

Rho-GTPase activity assays

After primary coculture with primary CLL cells, healthy donor T cells (10^7cells at a 2:1 ratio) were isolated by negative selection and starved for 5 hours (RPMI 1640 medium containing 1% serum) and then incubated with anti-CD3/CD28 T-Activator Dynabeads following the manufacturer's instructions (1:1 bead-to-cell ratio). After 45 minutes, T cells were harvested using a magnet to remove the beads before being lysed (100 μL of lysis buffer plus protease inhibitor cocktail) and RhoA, Rac1A, and Cdc42 activity was measured (490 nm colorimetric detection) according to the manufacturer's protocols (BK124, BK128, and BK127 G-LISA kits; Cytoskeleton).

Lenalidomide treatment

Lenalidomide was a kind gift from Celgene. Drug powder was dissolved in DMSO to make a 10mM stock and added to coculture assays or pretreatment of tumor cells at a 1μM final concentration in full culture medium (5nM for the treatment of RPMI8226 multiple myeloma [MM] cells). Vehicle control–treated cells were cultured using DMSO alone.

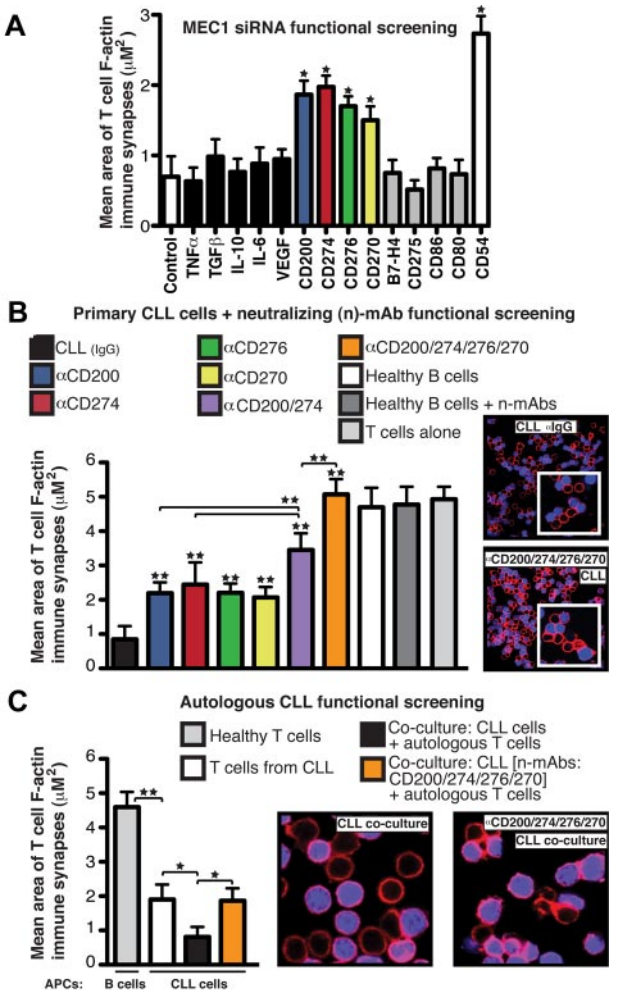

Figure 1. CD200, CD274, CD276, and CD270 mediate F-actin polymerization dysfunction at the T-cell synapse in CLL. (A) Mean synapse area ± SD from 6 healthy donor allogeneic T-cell functional screens with siRNA-treated MEC1 cells, with selected target molecules on the x-axis. CD54 siRNA and nontargeting siRNA (Control) treated cells acted as positive and negative controls, respectively. (B) Mean T-cell F-actin synapse area ± SD from 20 CLL patient cells pretreated with neutralizing Abs (α) before primary coculture with healthy donor allogeneic T cells. T cells were then negatively selected and used in conjugation assays with sAg-pulsed third-party healthy donor allogeneic B cells as APCs. (C) Mean T-cell synapse area ± SD from 6 CLL patient autologous functional screens. T cells from CLL patients were cocultured with autologous CLL cells. T cells were then negatively selected and used in conjugation assays with autologous CLL cells pulsed with sAg as APCs. T-cell/CLL(+sAg) and age-matched healthy donor T-cell/B cell (+sAg) autologous conjugates without primary coculture were included as controls. $^*P < .05$; $^{**}P < .01$. The confocal images show T-cell/APC conjugates after primary coculture with treated tumor cells. Original magnification, 63×.

Statistical methods

The Wilcoxon signed-rank test was used to compare repeated and paired measurements between 2 experimental groups. Multiple group comparisons were performed using repeated measures ANOVA (Friedman test) with a Dunn posttest for comparison of individual groups. We compared the data shown in Figures 2 and 3A and B using the Mann-Whitney test. The 2-tailed paired Student *t* test was used for the data shown in Figure 5. $P < .05$ was considered significant. All statistical analysis was done using Prism Version 5 software.

Results

Combined action of CLL-inhibitory ligands CD200, CD274, CD276, and CD270 suppress both allogeneic and autologous T-cell actin synapses

We designed a small interfering RNA (siRNA) functional synapse bioassay (supplemental Figure 1, available on the *Blood* Web site; see the Supplemental Materials link at the top of the online article) using the B-cell leukemia cell line MEC1,[15] which induces the same T-cell immune synapse defect as primary CLL cells,[6] and customized siRNA libraries that included soluble and membrane-immunosuppressive molecules.[16,17] siRNA-treated MEC1 cells were cocultured with healthy donor allogeneic T cells, which were subsequently used in conjugation assays with sAg-pulsed third-party, healthy donor allogeneic B cells as APCs. F-actin polymerization was quantified using confocal image analysis software. In this bioassay, knockdown of inhibitory molecules should lead to gain in function. Treatment of MEC1 cells with siRNA targeting soluble factors including TNFα, TGFβ, IL-10, or IL-6 did not increase T-cell F-actin polarization, which is consistent with our previous data showing that CLL-soluble factors did not induce this effect.[6] Knockdown of cell-surface molecules, including VEGF, B7-H4, CD275 (ICOS-L), CD86, or CD80 had no influence on F-actin polymerization, but we identified 3 B7 superfamily–related ligands[18-20]; CD200, CD274 (PD-L1), and CD276 (B7-H3); and 1 TNF-receptor superfamily member,[21] CD270 (HVEM or TNFRSF14), for which siRNA treatment of MEC1 cells enhanced immune synapse formation significantly (Figure 1A).

We confirmed these results using primary CLL cells from 20 untreated patients pretreated with individual or pooled neutralizing Abs before coculture with healthy donor allogeneic T cells. Blocking the combined activity of CD200, CD270, CD274, and CD276 increased F-actin synapse polymerization with APCs compared with individual neutralization or isotype control experiments (Figure 1B), whereas no effect was seen in healthy B cells with or without neutralizing Abs. CLL patients were selected to represent the heterogeneity of the disease including different Rai stages (I-III) and immunoglobulin variable heavy chain mutation status (mutated and unmutated; data not shown).[22-24] None of these factors was associated with extent of B7-related ligand immunosuppressive signaling activity. Additional siRNA knockdown experiments targeting these inhibitory ligands on primary CLL cells confirmed the inhibitory role of these molecules in mediating the T-cell synapse defect (supplemental Figure 1C). We showed previously that after coculture with CLL cells, previously healthy T cells exhibit a reduced ability to form conjugates with APCs and exhibit reduced polarization of key signaling molecules, including tyrosine-phosphorylated proteins, to the synapse. These defects lead to suppressed proliferation, cytokine release, and cytotoxic function.[6] Our screening results showed that blockade of tumor-inhibitory ligand signaling augmented T-cell synapse activities, including increased number of T-cell conjugates, phosphotyrosine expression, and function (data not shown). To identify the inhibitory coreceptors on T cells that receive the tumor immunosuppressive signaling, we performed reverse functional screening assays. These assays showed that Ab blockade of the T-cell counter-receptors CD200 receptor (CD200R), CD272 (BTLA), and CD279 (PD-1) before coculture with CLL cells also prevented the inhibitory ligand signaling, leading to significant gain in T-cell synapse and CTL effector function (supplemental Figure 2). We next verified an inhibitory role of these inhibitory ligands on autologous T cells from CLL patients, which exhibit impaired immune synapse formation with autologous CLL cells compared with age-matched healthy donor cells (synapse quantification of healthy T cells conjugated with sAg-pulsed autologous B cells; Figure 1C).[6] As shown in Figure 1C, autologous functional screening assays showed that direct contact coculture of T cells from CLL patients with autologous tumor cells in the absence of antigenic stimulation augmented defective synapse F-actin polymerization. However, pretreatment of CLL cells with neutralizing Abs targeting inhibitory ligands prevented this defect.

Inhibitory molecules are up-regulated in CLL and linked to poor prognosis

We also analyzed in situ expression of inhibitory ligands and their TCRs by IHC using a CLL lymph node TMA. Significantly higher expression of CD200, CD270, CD274, and CD276 on CD20$^+$ cells

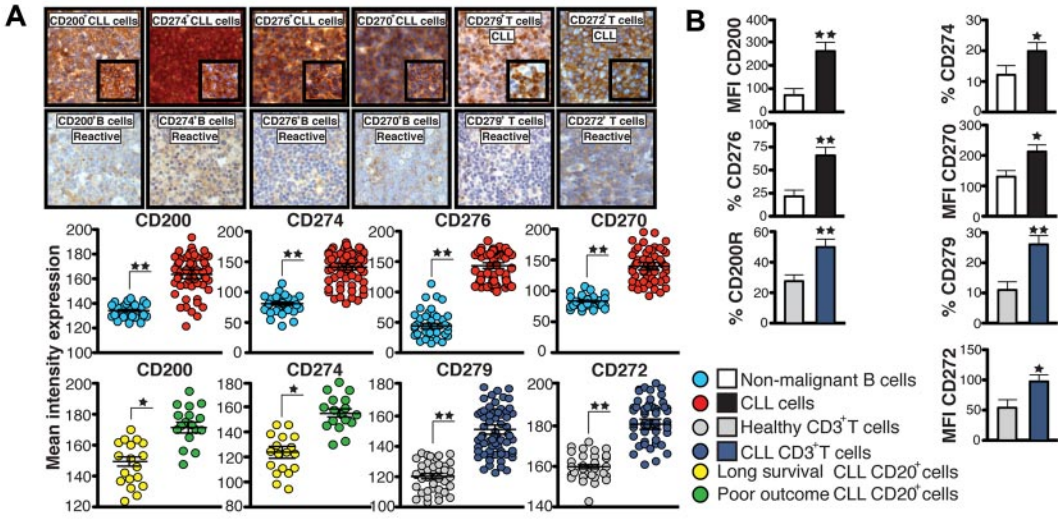

Figure 2. Inhibitory molecules are up-regulated in CLL cells and linked to poor patient prognosis. (A) IHC mean intensity expression analysis ± SEM of CD200, CD274, CD276, CD270 on CD20$^+$ cells, and CD279 and CD272 expression on CD3$^+$ T cells in CLL patient samples compared with reactive lymph node samples. Representative high-power 40× magnification and 63× inset images are shown. (B) MFI or percent positive expression analysis of inhibitory ligands and receptors on peripheral blood CD19$^+$ cells (CLL cells compared with healthy B cells) or autologous CD3$^+$ T cells from CLL patients or age-matched healthy donors. Columns show the means ± SEM from 12 patients. *$P < .05$; **$P < .01$.

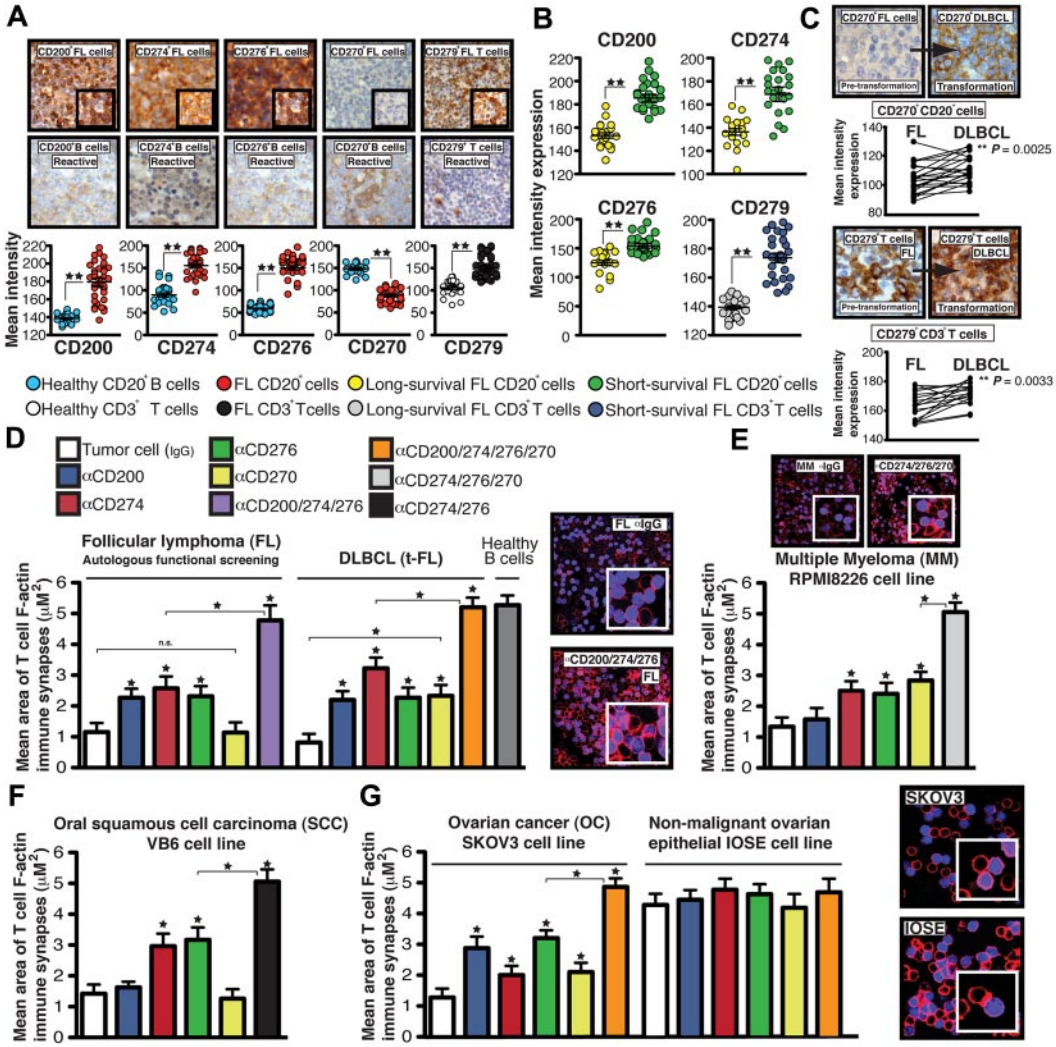

Figure 3. Tumor-induced T-cell actin synapse dysfunction mediated by inhibitory ligands is a common immunosuppressive mechanism used by hematologic and solid carcinoma cells. (A) IHC mean intensity expression ± SEM of CD200, CD274, CD276, and CD270 on intrafollicular CD20$^+$ cells and CD279 expression on interfollicular CD3$^+$ T cells in lymph tissue from FL patient samples compared with reactive lymph node samples (representative high-power 40× magnification and 63× inset images are shown). (B) Mean expression analysis ± SEM using an extremes of survival diagnostic FL TMA (>15-year long survival group compared with < 5-year short-survival patient group). (C) Representative high-power 40× magnification of CD270 expression on CD20$^+$ tumor cells and CD279 expression on CD3$^+$ T cells in TMA cores from pretransformation (FL) biopsy compared with each patient's transformation (DLBCL) biopsy. Comparison of expression between FL and transformation to DLBCL. (D) Autologous patient peripheral blood T-cell or healthy donor allogeneic T-cell F-actin synapse function with third-party healthy donor allogeneic B cells (+sAg) as APCs after primary coculture (24 hours) with primary tumor-infiltrated FL cells or DLBCLs (D), MM cell line RPMI8226 (E), SCC cell line VB6 (F), OC cell line SKOV3 (G) or a nonmalignant human ovarian epithelial cell line IOSE pretreated with neutralizing Abs (α). Colored columns show the mean T-cell synapse area ± SD from 6 donor functional screens. The confocal images show T-cell/APC conjugates after primary coculture with treated tumor cells (minimum n = 100 analyzed per experiment). Original magnification, 63×. *P < .05; **P < .01.

and CD272 and CD279 on CD3$^+$ T cells was seen in CLL samples compared with reactive lymph node samples. Significantly increased expression of CD200 and CD274 on CLL cells (Figure 2A) and CD279 on CD3$^+$ T cells (supplemental Figure 3A) was found in poor-prognosis patients (median survival, 38 months) compared with good-prognosis patients (median survival, > 10 years). Flow cytometric analyses of peripheral blood cells from CLL patients showed that all 4 inhibitory ligands were up-regulated on circulating CLL cells and their receptors on autologous T cells compared with age-matched healthy donor cells (Figure 2B and supplemental Figure 3B). The number of cells showing positive (%) expression for inhibitory molecules CD274, CD276, CD200R, and CD279 was significantly greater in CLL patients compared with healthy donors. In contrast, all cells expressed CD200, CD270, and CD272, but these had up-regulated expression levels (MFI) in CLL patients compared with healthy donors. These results identify up-regulated inhibitory molecules coopted by CLL tumor cells that mediate inhibitory-receptor–dependent T-cell synapse dysfunction.

Impairment of T-cell actin dynamics is a common immunosuppressive strategy in both hematologic and solid carcinoma cells

Similar F-actin polymerization synapse defects occur in FL tumor-infiltrating T cells, suggesting a common immunosuppressive pathway in hematologic malignancy.[13] IHC analysis of the inhibitory ligands and their receptors in diagnostic FL TMAs demonstrated increased expression of CD200, CD274, and CD276, but not CD270, on intrafollicular FL cells compared with reactive lymph tissue, as well as increased expression of CD279 on interfollicular T cells (Figure 3A). There was significantly higher expression of these molecules in poor- compared with good-prognosis patients (Figure 3B). In a separate transformation

(t-FL) TMA, increased expression of CD270 on lymphoma cells and CD279 on T cells was associated with transformation to DLBCL compared with paired pretransformation FL samples (Figure 3C). Blocking CD200, CD274, and CD276 on FL cells before coculture with autologous peripheral blood healthy T cells (nonleukemic phase disease) or healthy donor allogeneic T cells prevented induction of T-cell F-actin synapse defects. Transformed FL also used these inhibitory ligands, including CD270, during immunosuppressive signaling interaction with healthy donor allogeneic T cells (Figure 3D and supplemental Figure 4A-B).

We then broadened our analyses to other cancers. The MM cell line RPMI8226 and Hodgkin lymphoma cell lines (data not shown) express these inhibitory ligands and induce T-cell F-actin dysfunction in previously healthy allogeneic T cells after direct contact coculture (Figure 3E), whereas this was less marked with cell lines that did not express high levels of these inhibitory ligands (supplemental Figure 4C-D). The squamous cell carcinoma (SCC) cell line VB6[9] and the ovarian cancer (OC) cell line SKOV3[25] induced F-actin polymerization dysfunction in previously healthy allogeneic T cells. Functional data showed that these tumor cells use the same inhibitory ligand signaling axes as hematologic malignant cells (Figure 3F-G), whereas the nonmalignant ovarian epithelial cell line IOSE[10] had decreased expression of inhibitory ligands and did not modulate T-cell F-actin synapse function (Figure 3G and supplemental Figure 4E). These data suggest that both hematologic and solid cancer cells use common immunosuppressive-inhibitory mechanisms to suppress T-cell function.

The immunomodulatory drug lenalidomide prevents induction of tumor-induced T-cell lytic synapse dysfunction

The immunomodulatory drug lenalidomide is clinically active in CLL and lymphoma[26,27] and repairs autologous T-cell synapse formation defects in CLL, acting on immune cells and cancer cells.[6] The results presented in Figure 4A reveal blocking the ability of tumor cells to induce T-cell tolerance as a novel activity of this drug. In the present study, lenalidomide treatment blocked CLL cell–induced T-cell actin synapse dysfunction, mimicked Ab blockade experiments, and down-regulated expression of CLL inhibitory ligands and their receptors on T cells (Figure 4B and supplemental Figure 5A). Lenalidomide treatment (ie, pretreatment of CLL cells or direct addition of the drug to primary coculture) prevented tumor-induced immune suppression in FL, DLBCL, Hodgkin lymphoma (data not shown), MM, SCC, and OC cells and down-regulated immunosuppressive ligand expression on all tumor cells examined (Figure 4C and supplemental Figure 5B). CTL killing function increased significantly after Ab blockade of CLL-inhibitory ligands or lenalidomide treatment compared with control treatments (Figure 4D). Moreover, treatment of autologous CLL/T-cell cocultures with lenalidomide reversed impaired $CD8^+$ T-cell lytic synapse formation and granzyme B trafficking (Figure 4E). Direct clinical relevance of our findings was shown by analysis of CLL patient samples during an in vivo lenalidomide clinical trial that identified down-regulated inhibitory ligands (Figure 5C), increased T-cell conjugation and synapse function with autologous tumor cells acting as APCs (Figure 5A-B), and increased Ag-induced CTL effector activity with drug treatment (Figure 5D). Ex vivo coculture of CLL cells that had been treated with lenalidomide with autologous T-cell populations in the absence of drug did not induce any detectable induction of T-cell tolerance, suggesting stable immunomodulatory activity.

Tumor-inhibitory signaling targets T-cell Rho-GTPase activation signaling that is reversible with lenalidomide or Ab blockade

To gain insight into the molecular targets of tumor-induced T-cell actin dysregulation, we measured T-cell expression of activated, GTP-bound Rho family members that regulate actin polymerization.[28] Consistent with previous studies, we found that engagement of the TCR in healthy T cells elicits a complex cascade of signaling events that regulate the activation and location of RhoA, Rac1, and Cdc42 Rho-GTPases (Figure 6).[29] Increased Rac1 activation at the front of the T cell is linked to dynamic lamellipodium structures that form the actin-rich synapse. In contrast, TCR-induced uropod disappearance is associated with profound arrest of RhoA activity at the back of the T cell. However, activated RhoA and Cdc42 are located at the synapse site. Therefore, stimulation of T cells through the TCR specifically activates RhoA, Rac1, and Cdc42 at the immune synapse.[30] It has been proposed that these signaling mechanisms allow T-cell retention and synapse formation on Ag recognition. As can be seen in Figure 6, coculture with CLL cells decreased activated RhoA, Rac1, and Cdc42 levels in TCR-stimulated T cells significantly compared with age-matched healthy B cells. These tumor-exposed T cells also showed reduced myosin activity that has been shown to regulate TCR signaling and immune synapse stability (supplemental Figure 6).[31] In contrast, Ab blockade of CLL-inhibitory ligand signaling or lenalidomide treatment prevented induction of these T-cell Rho-GTPase signaling defects in previously healthy donor T cells (Figure 6).

Discussion

$CD4^+$ and $CD8^+$ T cells are critical for controlling immune function, including immune surveillance of tumor cells. There is currently a renewed optimism and realization that immune-based therapies have the potential to make significant clinical contributions toward the treatment of incurable cancers and target drug-resistant tumor subclones.[2,32,33] However, clinical-grade therapies such as adoptive cell transfer can involve complicated and very expensive ex vivo manipulations. In addition to this translational cost barrier, it is now becoming recognized that cancer cells actively use immune evasion mechanisms to combat immune function. This is an emerging hallmark of cancer biology, and this pro-tumor microenvironment is likely to be a major biologic barrier to the success of immunotherapy protocols such as transplantation, adoptive cell transfer, and vaccination.[3,13] We have previously defined a common immune defect in CLL and lymphoma: an inability of tumor-exposed T cells to form functional immune synapses with APCs. Of clinical relevance, we also showed that the immunomodulatory drug lenalidomide repaired this autologous defect by restoring T-cell actin activation signaling and enhancing APC function of tumor B cells.[6,13]

In the present study, we screened siRNA libraries and used a functional synapse bioassay to identify the molecules and signaling mechanisms with which tumor cells induce T-cell synapse defects. We have shown herein that the inhibitory B7-related molecules CD200, CD274 (PD-L1), and CD276 (B7-H3) and the TNF-receptor superfamily member CD270 (HVEM) are highly expressed on leukemic cells and are key mediators of the global T-cell synapse defect (Figure 1). We also showed that CD200R, CD279 (PD-1), and CD272 (BTLA) are the T cell–inhibitory coreceptors that transmit tumor immunosuppressive signaling (supplemental

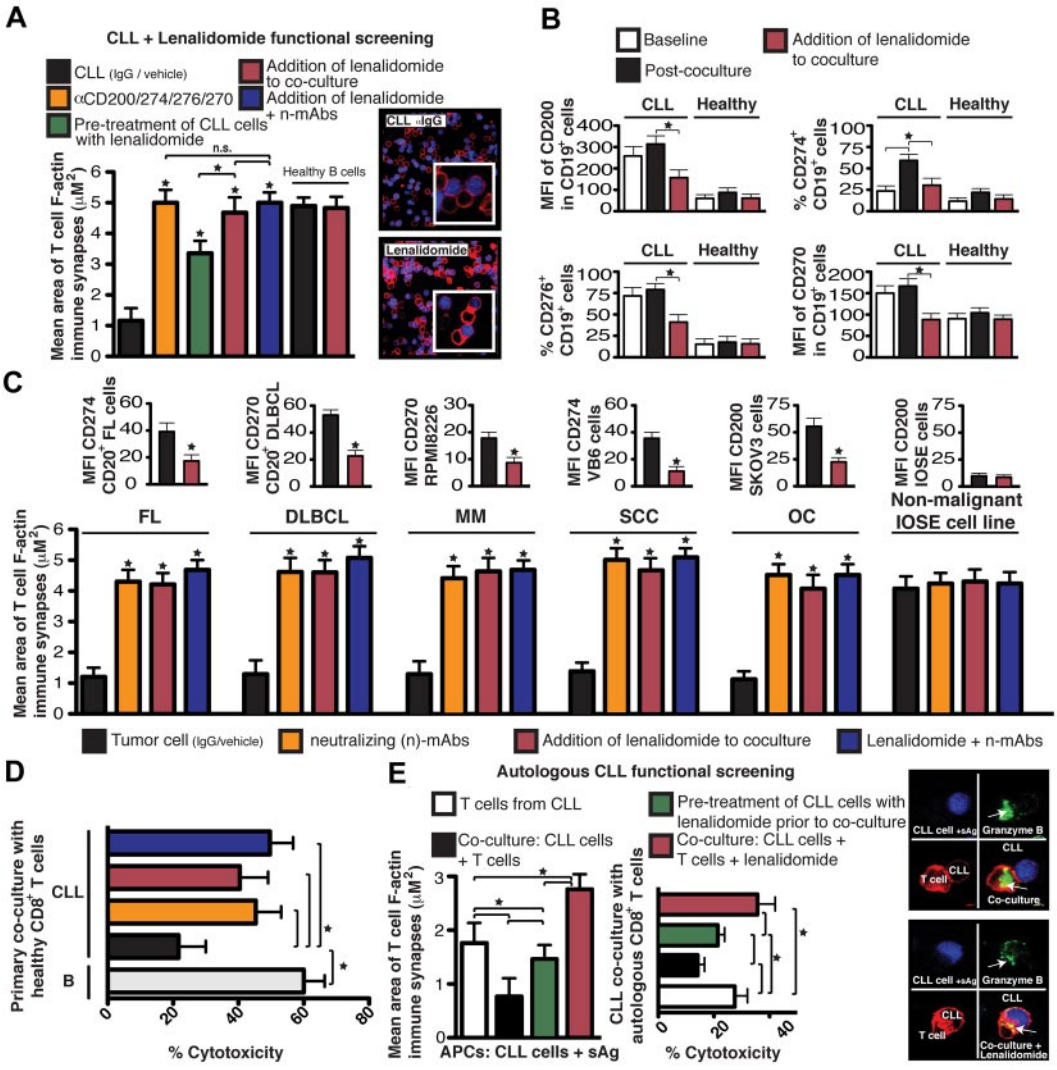

Figure 4. Lenalidomide down-regulates tumor-inhibitory ligand expression and prevents tumor-induced lytic synapse dysfunction. (A,C) Healthy donor allogeneic T-cell synapse function with third-party healthy donor allogeneic B cells (+sAg) as APCs after primary coculture with primary CLL cells (A) primary FL and DLBCL cells (autologous patient peripheral blood T cells; C), MM cell line RPMI8226, SCC cell line VB6, OC cell line SKOV3 or nonmalignant IOSE cell line treated with neutralizing Abs (n-mAbs, α) and/or lenalidomide (1μM). Mean F-actin synapse area ± SD from 6 donor functional screens. MFI expression data (mean ± SEM from 6 independent experiments) before and after 24 hours of exposure to lenalidomide is also shown. (B) FACs MFI or percent positive expression of CD200, CD274, CD276, and CD270 on CD19⁺ CLL cells or age-matched CD19⁺ healthy donor B cells before (baseline) and after coculture (48 hours) with third-party healthy donor allogeneic T cells in the presence of vehicle control or lenalidomide (1μM). Columns show the mean plusmn] SEM from 6 coculture experiments. (D) Healthy donor CTL killing function using third-party healthy donor allogeneic B cells (+sAg) as APCs after primary coculture (48 hours) with CLL cells or age-matched CD19⁺ healthy donor allogeneic B cells. Mean percent cytotoxicity of each treatment ± SD from 6 CLL patient functional screens is shown. (E) Mean CD8⁺ T-cell synapse area and percent cytotoxicity ± SD from 6 CLL patient autologous functional screens using CLL cells pulsed with sAg as APCs. Autologous T cell–CLL(+sAg) conjugates or CTL cells alone without primary coculture were included as controls (white columns). *$P < .05$. The confocal images show T-cell/APC conjugate populations after primary coculture. Original magnification, 63×.

Figure 2). CLL cells exploit the combined action of these multiple coinhibitory ligand-receptor signaling axes to induce T-cell F-actin synapse dysfunction and suppress effector function in both previously healthy allogeneic and autologous patient T-cell populations. Mechanistically, this tumor-inhibitory signaling down-regulates activated Rho-GTPases RhoA, Rac1, and Cdc42, key regulators of T-cell synapse actin dynamics (Figure 6).[30,34] TCR-stimulation specifically activates RhoA, Rac1, and Cdc42 at the immune synapse, and we postulate that tumor-cell modulation of Rho-activation signaling accounts for the global T-cell immune synapse and functional defects in CLL. These data are consistent with our initial observation that actin cytoskeletal signaling pathways are dysregulated profoundly in both the CD4⁺ and CD8⁺ T-cell populations in CLL.[4] The specific delineation of the downstream signaling mechanisms, including the small GTPases that are affected by cancer cell engagement of the T-cell inhibitory receptors, is the subject of our ongoing studies. In the present study, we identified a novel immunomodulatory mechanism of action of lenalidomide: blocking tumor-cell–induced T-cell synapse dysfunction (Figures 4 and 5). Both ex vivo and in vivo lenalidomide treatment prevents induction of the T-cell defect and down-regulates increased expression of inhibitory ligands on tumor cells and their receptors on T cells. The discovery that lenalidomide can block the induction of cancer-cell–induced T-cell tolerance, together with our previous observation that it can repair the autologous T-cell synapse defect present in cancer patients, provides important mechanism of action data for the observed clinical activity of this agent in ongoing clinical trials.[6,26] The ability of this drug to promote T-cell activity and reeducate existing T-cell populations in cancer patients represents a very attractive immunomodulatory strategy. These findings suggest that lenalidomide should be considered in combination with other immunotherapies,

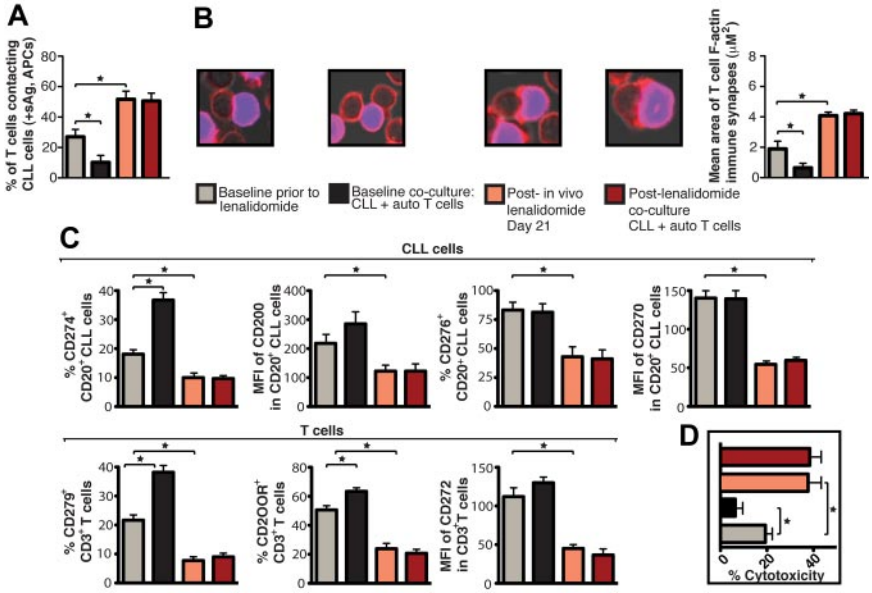

Figure 5. Lenalidomide in vivo treatment enhances patient T-cell F-actin polymerization at the immunologic synapse with autologous tumor APCs, down-regulates expression of CLL cell inhibitory ligands and T-cell inhibitory receptors, and increases autologous CTL effector function. CD19⁺ CLL cells and T cells (CD3⁺ and CD8⁺) were purified from both pretreatment baseline and after lenalidomide treatment (day 21) samples and used in subsequent analysis. These purified cells were also used in paired ex vivo autologous (auto) coculture experiments (48 hours) with subsequent functional and flow cytometric analysis. (A) Quantification of CD3⁺ T cells in contact with autologous CLL cells (pulsed with sAg acting as APCs) by immunofluorescence. (B) Mean percent T-cell conjugation ± SD from 3 CLL patients. CD3⁺ T cell–CLL cell (+sAg) conjugates (n = 100 per experiment) were analyzed for the area (μM^2) of F-actin polymerization at the synapse contact site. Mean synapse area ± SD from 3 CLL patients. The confocal images show representative T-cell synapses for each treatment. Original magnification, 63×. (C) Purified CLL cells and CD3⁺ T cells were examined for inhibitory ligand and receptor expression, respectively, by FACS analysis. Columns show the mean MFI or percent positive expression ± SEM from 3 CLL patients. (D) Mean percent CD8⁺ T-cell cytotoxicity of autologous CLL cells (+sAg) ± SD from 3 CLL patients (effector-to-target ratio, 30:1) comparing pretreatment baseline and after lenalidomide treatment samples. *$P < .05$.

including existing clinical-grade antagonist Abs that target inhibitory molecules such as CD279 (PD-1)/CD274 (PD-L1), and CD276 (B7-H3).[33]

Our previous work has shown that the profound molecular and functional synapse defects observed in T cells after CLL or FL tumor-cell coculture are global.[4,6,8,13] These defects are not restricted to Ag-specific responses nor are they repaired by the addition of exogenous IL-2, features that might be expected in anergic cells. We have not been able to demonstrate any involvement of regulatory T cells in the observed immune synapse defect. Our combined data point to global T-cell suppression via receptor-based immune evasion by cancer cells. Support for the use of CLL as a model comes from our results in other hematologic malignancies (eg, FL and DLBCL) and solid epithelial cancer cell lines (eg, OC and SCC) that show strong expression and immunosuppressive activity of these inhibitory molecules compared with nonmalignant control cells (Figure 3). This potent inhibitory activity toward previously healthy donor T cells mediated by epithelial tumor cells that lack the same MHC expression profile as tumor B cells suggests that cancer cells "hijack" immune-regulatory molecules that are normally tightly regulated on healthy APCs. We have also demonstrated that primary FL tumor cells derived from lymph node biopsies induce T-cell synapse dysfunction in previously healthy autologous peripheral blood T-cell populations (ie, nonleukemic phase disease patients) and healthy donor allogeneic T cells via up-regulated CD200-, CD274-, and CD276-inhibitory signaling. We have demonstrated the utility of antagonist Ab blockade or lenalidomide treatment in down-regulating the activity of these immunosuppressive signaling axes in our functional synapse bioassay (Figure 4). Our findings are supported by other studies showing that primary mediastinal lymphoma B cells overexpress CD274, which induces T-cell activation defects after short-term primary coculture.[35] Blocking CD274 on anaplastic large-cell lymphoma cells prevented the induction of impaired IFN-γ and proliferation responses in previously healthy allogeneic T-cell and autologous tumor–associated T-cell populations.[36] Of clinical importance, lenalidomide has been shown to down-regulate CD274 expression on primary MM cells.[37] The relevance of our findings to acute leukemias has also been highlighted by a recent study describing up-regulated CD274 expression on acute lymphoblastic leukemia tumor cells as driving the induction of inhibitory receptor CD279 expression on previously healthy naive T-cell populations

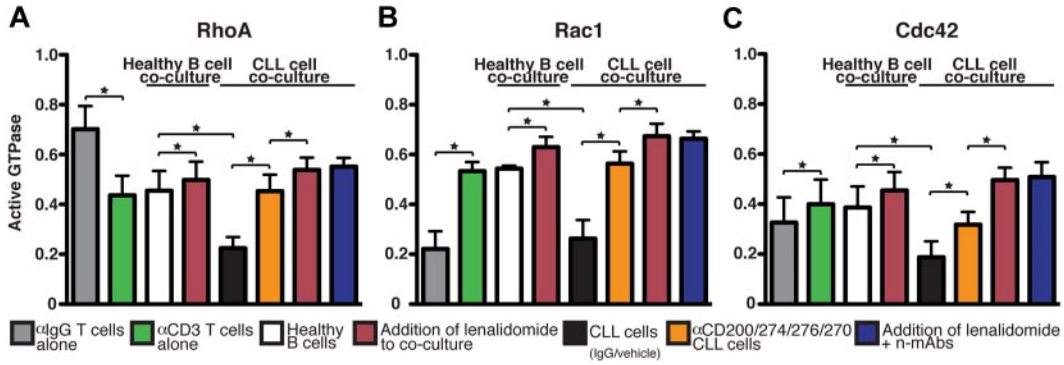

Figure 6. CLL-immunosuppressive signaling targets Rho-GTPase activation signaling that is reversible with lenalidomide or Ab blockade. Healthy donor allogeneic T cells after primary coculture (48 hours) with treated primary CLL cells (or third-party healthy donor allogeneic B cells) were starved for 5 hours and then incubated with anti–(α)-CD3/CD28 beads. After 45 minutes, cells were lysed and T-cell RhoA (A), Rac1 (B), and Cdc42 (C) activity was measured using G-LISA assays (absorbance at 490 nm). Colored columns show the combined mean activation signal ± SD from 6 CLL patient functional screens. Healthy donor T cells treated alone with CD3/CD28 or control IgG beads were included as controls. *$P < .05$.

in a murine model of disease.[38] We have observed a similar rapid induction of global synapse functional defects in T cells from young, healthy mice that were infused with CLL tumor cells.[8] We conclude that tumor cell–induced impaired actin polymerization mediated by abnormal cancer-specific inhibitory ligand signaling is a common T-cell defect in human cancer. These results also suggest that hematologic malignancies are good models with which to study this cancer immune evasion mechanism because of the intrinsic increased exposure of T cells to these tumor-immunosuppressive signaling interactions.

Opposing activating and inhibitory B7-related molecules modulate TCR-mediated signaling in normal T-cell/APC immune interactions.[39] The expression of inhibitory ligands are up-regulated in many cancer types,[16,40-42] and this is linked to poor patient prognosis.[43] However, the mechanistic consequences of this abnormal expression have not been fully defined previously. In the present study, we show that, in contrast to healthy cells, tumor cells express high levels of B7-related inhibitory ligands and exploit their function and affinity for their receptors to induce impaired T-cell F-actin synapse formation and CTL effector function. Our future studies will focus on comparing this inhibitory signaling in cancer cells with healthy APCs using established models for measuring lymphocyte activation.[44] Our data show that dysregulated Rho-GTPase signaling is a major target pathway for understanding and repairing tumor cell–induced T-cell defects. The identification of CD200, CD270, CD274, and CD276 proteins as key molecules in cancer immune suppression provides new molecular targets for developing improved immunotherapy approaches in CLL and other malignancies to complement existing antitumor therapies.

Acknowledgments

The authors thank the patients and donors who consented to the use of their cell and tissue samples for this study; Dr Shah-Jalal Sarker (Center for Experimental Cancer Medicine Barts Cancer Institute, London) for statistical method advice; Dr Guglielmo Rosignoli for flow cytometry assistance; Dr Simon Joel for providing hematologic cell lines; and Professor Fran Balkwill and Dr John Marshall for providing the SKOV3 and VB6 cell lines, respectively.

This research was funded by the European Hematology Association (fellowship grant 2009/16 to A.G.R.) and by program grants from the National Cancer Institute, National Institutes of Health, to the CLL Research Consortium (P01 CA81538 to J.G.G.) and from Cancer Research UK (C1574/A6806).

Authorship

Contribution: A.G.R. designed, performed, and supervised the experiments and data analysis and wrote the manuscript; A.J.C. performed and analyzed the IHC experiments; R.F. assisted with the experiments and data analysis; and J.G.G. designed and supervised the experiments and wrote the manuscript.

Conflict-of-interest disclosure: J.G.G. has received honoraria from Celgene for work on advisory boards. The remaining authors declare no competing financial interests.

Correspondence: Alan G. Ramsay, Barts Cancer Institute, Centre for Haemato-Oncology, Charterhouse Square, London EC1M 6BQ, United Kingdom; e-mail: a.ramsay@qmul.ac.uk.

References

1. Weiner LM, Surana R, Wang S. Monoclonal antibodies: versatile platforms for cancer immunotherapy. *Nat Rev Immunol.* 2010;10(5):317-327.
2. Porter DL, Levine BL, Kalos M, Bagg A, June CH. Chimeric antigen receptor-modified T cells in chronic lymphoid leukemia. *N Engl J Med.* 2011; 365(8):725-733.
3. Hanahan D, Weinberg RA. Hallmarks of cancer: the next generation. *Cell.* 2011;144(5):646-674.
4. Görgün G, Holderried TA, Zahrieh D, Neuberg D, Gribben JG. Chronic lymphocytic leukemia cells induce changes in gene expression of CD4 and CD8 T cells. *J Clin Invest.* 2005;115(7):1797-1805.
5. Dustin ML, Depoil D. New insights into the T cell synapse from single molecule techniques. *Nat Rev Immunol.* 2011;11(10):672-684.
6. Ramsay AG, Johnson AJ, Lee AM, et al. Chronic lymphocytic leukemia T cells show impaired immunological synapse formation that can be reversed with an immunomodulating drug. *J Clin Invest.* 2008;118(7):2427-2437.
7. Dustin ML, Long EO. Cytotoxic immunological synapses. *Immunol Rev.* 2010;235(1):24-34.
8. Gorgun G, Ramsay AG, Holderried TA, et al. E(mu)-TCL1 mice represent a model for immunotherapeutic reversal of chronic lymphocytic leukemia-induced T-cell dysfunction. *Proc Natl Acad Sci U S A.* 2009;106(15):6250-6255.
9. Ramsay AG, Keppler MD, Jazayeri M, et al. HS1-associated protein X-1 regulates carcinoma cell migration and invasion via clathrin-mediated endocytosis of integrin alphavbeta6. *Cancer Res.* 2007;67(11):5275-5284.
10. Li NF, Broad S, Lu YJ, et al. Human ovarian surface epithelial cells immortalized with hTERT maintain functional pRb and p53 expression. *Cell Prolif.* 2007;40(5):780-794.
11. Proto-Siqueira R, Panepucci RA, Careta FP, et al. SAGE analysis demonstrates increased expression of TOSO contributing to Fas-mediated resistance in CLL. *Blood.* 2008;112(2):394-397.
12. Lee AM, Clear AJ, Calaminici M, Macdougall F, Goff L, Gribben JG. Increased CD68 and decreased CD4 expressing cells in tissue microarray (TMA) in diagnostic lymph node biopsies are associated with poor outcome in CLL/SLL [abstract]. *Blood (ASH Annual Meeting Abstracts).* 2006;108(11):2781.
13. Ramsay AG, Clear AJ, Kelly G, et al. Follicular lymphoma cells induce T-cell immunologic synapse dysfunction that can be repaired with lenalidomide: implications for the tumor microenvironment and immunotherapy. *Blood.* 2009;114(21): 4713-4720.
14. Davies AJ, Rosenwald A, Wright G, et al. Transformation of follicular lymphoma to diffuse large B-cell lymphoma proceeds by distinct oncogenic mechanisms. *Br J Haematol.* 2007;136(2):286-293.
15. Stacchini A, Aragno M, Vallario A, et al. MEC1 and MEC2: two new cell lines derived from B-chronic lymphocytic leukaemia in prolymphocytoid transformation. *Leuk Res.* 1999;23(2):127-136.
16. Zou W, Chen L. Inhibitory B7-family molecules in the tumour microenvironment. *Nat Rev Immunol.* 2008;8(6):467-477.
17. Zou W. Immunosuppressive networks in the tumour environment and their therapeutic relevance. *Nat Rev Cancer.* 2005;5(4):263-274.
18. Coyle AJ, Gutierrez-Ramos JC. The expanding B7 superfamily: increasing complexity in costimulatory signals regulating T cell function. *Nat Immunol.* 2001;2(3):203-209.
19. Kretz-Rommel A, Qin F, Dakappagari N, et al. CD200 expression on tumor cells suppresses antitumor immunity: new approaches to cancer immunotherapy. *J Immunol.* 2007;178(9):5595-5605.
20. Keir ME, Butte MJ, Freeman GJ, Sharpe AH. PD-1 and its ligands in tolerance and immunity. *Annu Rev Immunol.* 2008;26:677-704.
21. Paulos CM, June CH. Putting the brakes on BTLA in T cell-mediated cancer immunotherapy. *J Clin Invest.* 2010;120(1):76-80.
22. Chiorazzi N, Rai KR, Ferrarini M. Chronic lymphocytic leukemia. *N Engl J Med.* 2005;352(8): 804-815.
23. Kay NE, O'Brien SM, Pettitt AR, Stilgenbauer S. The role of prognostic factors in assessing 'high-risk' subgroups of patients with chronic lymphocytic leukemia. *Leukemia.* 2007;21(9):1885-1891.
24. Zenz T, Mertens D, Kuppers R, Dohner H, Stilgenbauer S. From pathogenesis to treatment of chronic lymphocytic leukaemia. *Nat Rev Cancer.* 2010;10(1):37-50.
25. Hagemann T, Wilson J, Burke F, et al. Ovarian cancer cells polarize macrophages toward a tumor-associated phenotype. *J Immunol.* 2006; 176(8):5023-5032.
26. Chen CI, Bergsagel PL, Paul H, et al. Single-agent lenalidomide in the treatement of previously untreated chronic lymphocytic leukemia. *J Clin Oncol.* 2011;29(9):1175-1181.
27. Nowakowski GS, LaPlant B, Habermann TM, et al. Lenalidmide can be safely combined with R-CHOP (R2CHOP) in the intial chemotherapy for aggressive B-cell lymphomas: phase I study. *Leukemia.* 2011;25(12):1877-1881.
28. Vicente-Manzanares M, Sanchez-Madrid F. Role of the cytoskeleton during leukocyte responses. *Nat Rev Immunol.* 2004;4(2):110-122.
29. Cernuda-Morollón E, Millam J, Shipman M,

Marelli-Berg FM, Ridley AJ. Rac activation by the T-cell receptor inhibits T cell migration. *PLoS One.* 2010;5(8):e12393.

30. Singleton KL, Roybal KT, Sun Y, et al. Spatiotemporal patterning during T cell activation is highly diverse. *Sci Signal.* 2009;2(65):ra15.
31. Ilani T, Vasiliver-Shamis G, Vardhana S, Bretscher A, Dustin ML. T cell antigen receptor signaling and immunological synapse stability require myosin IIA. *Nat Immunol.* 2009;10(5):531-539.
32. Perl A, Carroll M. BCR-ABL kinase is dead; long live the CML stem cell. *J Clin Invest.* 2011;121(1):22-25.
33. Pardoll D, Drake C. Immunotherapy earns its spot in the ranks of cancer therapy. *J Exp Med.* 2012;209(2):201-209.
34. Burkhardt JK, Carrizosa E, Shaffer MH. The actin cytoskeleton in T cell activation. *Annu Rev Immunol.* 2008;26:233-259.
35. Steidl C, Shah SP, Woolcock BW, et al. MHC class II transactivator CIITA is a recurrent gene fusion partner in lymphoid cancers. *Nature.* 2011;471(7338):377-381.
36. Andorsky DJ, Yamada RE, Said J, Pinkus GS, Betting DJ, Timmerman JM. Programmed death ligand 1 is expressed by non-Hodgkin lymphomas and inhibits the activity of tumor-associated T cells. *Clin Cancer Res.* 2011;17(13):4232-4244.
37. Benson DM Jr., Bakan CE, Mishra A, et al. The PD-1/PD-L1 axis modulates the natural killer cell versus multiple myeloma effect: a therapeutic target for CT-011, a novel monoclonal anti-PD-1 antibody. *Blood.* 2010;116(13):2286-2294.
38. Burk CR, Fix W, Qin H, Fry TJ. ALL progression induces PD-1 on T cells and blockade of PD-1 enhances adoptive immunotherapy [abstract]. *Blood (ASH Annual Meeting Abstracts).* 2011;118(21):2587.
39. Sharpe AH. Mechanisms of costimulation. *Immunol Rev.* 2009;229(1):5-11.
40. Siva A, Xin H, Qin F, Oltean D, Bowdish KS, Kretz-Rommel A. Immune modulation by melanoma and ovarian tumor cells through expression of the immunosuppressive molecule CD200. *Cancer Immunol Immunother.* 2008;57(7):987-996.
41. Derre L, Rivals JP, Jandus C, et al. BTLA mediates inhibition of human tumor-specific CD8+ T cells that can be partially reversed by vaccination. *J Clin Invest.* 2010;120(1):157-167.
42. Katayama A, Takahara M, Kishibe K, et al. Expression of B7-H3 in hypopharyngeal squamous cell carcinoma as a predictive indicator for tumor metastasis and prognosis. *Int J Oncol.* 2011;38(5):1219-1226.
43. Hamanishi J, Mandai M, Iwasaki M, et al. Programmed cell death 1 ligand 1 and tumor-infiltrating CD8+ T lymphocytes are prognostic factors of human ovarian cancer. *Proc Natl Acad Sci U S A.* 2007;104(9):3360-3365.
44. Treanor B, Batista FD. Mechanistic insight into lymphocyte activation through quantitative imaging and theoretical modelling. *Curr Opin Immunol.* 2007;19(4):476-483.